

Relationship between the Indian monsoon rainfall and the tropospheric temperature over the Eurasian continent

By XIAODONG LIU and MICHIO YANAI*
University of California, USA

(Received 14 March 2000; revised 27 November 2000)

SUMMARY

Based on climatological data such as the all-India rainfall (AIR) for 1949–98, air temperatures in the troposphere and at the land surface for 1949–98 as well as precipitation and outgoing long-wave radiation (OLR) for 1979–98, the statistical relationship between the Indian monsoon rainfall and tropospheric temperature (TT) over the Eurasian continent is examined by using the correlation analysis and singular value decomposition (SVD) analysis methods. The main results are summarized as follows. (1) The June–September (JJAS) AIR has significant positive correlations with the 200–700 hPa TT averaged for Eurasia in JJAS. The area with the highest simultaneous correlation of upper TT with AIR for JJAS is located in western Eurasia. There is also a region with positive simultaneous correlations in the southern subtropics covering southern Africa. The JJAS AIR also shows significant positive correlations with TT over the Eurasian continent in March–May (MAM) and with the TT averaged over the Tibetan Plateau in September and October. Although some precursory springtime temperature signals for the anomalous summer monsoon are found in the upper TT over Eurasia, the variation in the upper TT appears mostly independent from that of the land surface temperature. (2) The anomalies of upper TT in JJAS are closely coupled with the variations in OLR related to the monsoon rainfall over tropical Asia and Africa. The spatial structure of the first SVD mode for OLR anomalies shows the coherent variations in convective activity from northern tropical Africa to India, while the pattern of the first SVD mode for 300 hPa temperature anomalies shows a distribution which is nearly symmetric with respect to the equator, with variations of the same sign over subtropical areas in both hemispheres and variations of the opposite sign around equatorial Africa. *This pair of coupled patterns suggests that when the monsoon rains from tropical Africa to India become more intense, the upper troposphere from northern Africa to western Asia and over southern Africa becomes warmer.* (3) The observed temperature variation in the upper troposphere over the Eurasian continent (especially western Eurasia) during the summer monsoon season is considered to be a result of the anomalous subsidence and thermal advection, dynamically induced by anomalous tropical heating associated with the enhanced monsoon rainfall. This study suggests that the tropical convective activity linked to the Indian monsoon rainfall has an impact on the atmospheric variability on a global scale.

KEYWORDS: Correlation Indian monsoon rainfall Singular value decomposition Tropospheric temperature

1. INTRODUCTION

The Asian summer monsoon is generally believed to result from the seasonal differential heating between the Eurasian land mass and the adjacent oceans (e.g. Webster *et al.* 1998). Many studies indicated that the Asian summer monsoon is influenced by the heating over the Eurasian continent, especially the Tibetan Plateau (the Qinghai-Xizang Plateau). On a seasonal time-scale, it is known that the onset of the Asian summer monsoon is concurrent with the reversal of meridional temperature gradient in the upper troposphere south of the Tibetan Plateau (Flohn 1957; Li and Yanai 1996) and closely related to the warming over the Tibetan Plateau (e.g. Yeh *et al.* 1957; Ueda and Yasunari 1998). Using the FGGE (First GARP (Global Atmospheric Research Program) Global Experiment) and QXPME (Qinghai-Xizang Plateau Meteorology Experiment) data, Yanai *et al.* (1992) showed that the onset of the Asian summer monsoon of 1979 was associated with the sensible heating from the surface of the Tibetan Plateau and the warming in the upper troposphere over the plateau from spring to summer. They also noted a substantial contribution from latent-heat release on the eastern Plateau in summer.

* Corresponding author: Department of Atmospheric Sciences, University of California, Los Angeles, 405 Hilgard Avenue, Los Angeles, CA 90095-1565, USA. e-mail: yanai@atmos.ucla.edu

However, only a few studies have examined the interannual variability of the Asian summer monsoon in relation to that of the land–sea thermal contrast. Fu and Fletcher (1985) found that the interannual variability of the Indian monsoon rainfall was highly correlated with the variability of thermal contrast between the Tibetan Plateau and the equatorial Pacific. Li and Yanai (1996) contrasted the strong and weak monsoon years during the period 1979–92 and showed the enhanced (weakened) land–sea thermal contrast in the upper troposphere during the summer months of the strong (weak) monsoon years. Considering the importance of thermal contrast between the mid-latitude land and the tropical Indian Ocean in maintaining the Asian monsoon system, Kawamura (1998) used the meridional gradient of summertime upper-tropospheric thickness (200–500 hPa) anomalies across 20°N over the Indian subcontinent to define an Asian summer monsoon index to measure the intensity of the monsoon and its interannual variations. Singh and Chattopadhyay (1998) examined the statistical relationship between Indian monsoon rainfall and tropospheric temperature (TT) anomalies over seven selected Indian stations. Their results indicated that the Indian monsoon rainfall has a strong and positive correlation with the preceding May TT anomaly. Nevertheless, the effect of the heating of the Tibetan Plateau or Eurasian continent on the interannual variability of the Asian summer monsoon has not been firmly established. Recently, several numerical experiments (Lau and Bua 1998; Shen *et al.* 1998; Watanabe and Nitta 1998; Yang and Lau 1998) showed that ocean basin-scale sea surface temperature (SST) anomalies exert a stronger control on the interannual variation of the monsoon than the land surface processes. Moreover, the land surface processes in winter and spring may have an influence only on the early part of the following summer monsoon (Yang and Lau 1998). Some modelling results even suggested that atmosphere–land interactions are not essential for the monsoon variability (Zwiers 1993; Lau and Nath 2000).

Most of the previous studies on TT and Indian monsoon rainfall focused on the possible influence of TT related to the land surface processes on the Indian monsoon rainfall, but rarely examined the role of the Indian monsoon rainfall in the TT variability. However, the activity of the Asian monsoon is believed to play an active part in the atmospheric interannual variability, especially the tropospheric biennial oscillation (Yasunari and Seki 1992; Meehl 1994, 1997). Rodwell and Hoskins (1996) proposed that the diabatic heating resulting from the Asian monsoon rainfall induces a Rossby-wave pattern to the west and eventually results in enhanced adiabatic descent and desertification over remote eastern Sahara and the Mediterranean.

In this study, we further examine the statistical relationship between the Indian monsoon rainfall and large-scale TTs mainly over the Eurasian continent including the Tibetan Plateau. We focus on the following three topics: (1) the simultaneous and lag correlations of the Indian monsoon rainfall with TT over Eurasia for both spring and summer; (2) the coupled relationship between the Asian–African monsoon rainfall pattern and temperature anomaly pattern; and (3) possible cause–effect chains of variations in the Indian monsoon rainfall and TT.

2. DATA AND METHOD

Data used in this study include: (1) monthly all-India rainfall (AIR) from rain-gauge stations for the period 1949–98 prepared by the Indian Institute of Tropical Meteorology (Mooley *et al.* 1981; Parthasarathy *et al.* 1987); (2) monthly Climate Prediction Center merged analysis of precipitation (CMAP) with a $2.5^\circ \times 2.5^\circ$ resolution for 1979–98 (Xie and Arkin 1997); (3) monthly mean values of $2.5^\circ \times 2.5^\circ$ resolution outgoing long-wave radiation (OLR) observed from the Advanced Very High Resolution Radiometer

(AVHRR) on the National Oceanic and Atmospheric Administration (NOAA) satellites for 1979–98; (4) monthly mean temperatures at 10 levels on a $2.5^\circ \times 2.5^\circ$ grid for the period 1949–98, and 200 hPa horizontal wind and 500 hPa vertical velocity data for 1979–98 from the National Centers for Environment Prediction (NCEP)–National Center for Atmospheric Research (NCAR) re-analysis (Kalnay *et al.* 1996); (5) monthly $5^\circ \times 5^\circ$ grid-box land-surface-temperature-anomaly dataset for 1949–98 provided by the Climatic Research Unit, University of East Anglia, UK (Jones 1994); (6) 1950–98 monthly SST anomaly series for the NINO3 region (5°N – 5°S , 150° – 90°W) prepared by the Climate Prediction Center, NOAA.

In the present study we use the correlation analysis to examine the simultaneous and time-lagged relationships between AIR and TT, and the singular value decomposition (SVD) method to reveal the coupled relationship between the Asian–African monsoon rainfall pattern and the temperature anomaly pattern. SVD is a powerful tool for identifying sets of linear relationships between two fields. The method is used to find relationships between the two fields by decomposing the covariance matrix of the two fields into singular values and two sets of paired orthogonal vectors, one for the ‘left’ field and one for the ‘right’ field. SVD maximizes the covariance between the expansion coefficients of the leading patterns in the left and right fields. A detailed description of SVD can be found in Bretherton *et al.* (1992) and Wallace *et al.* (1992). In addition, linear regression analyses are used to find the response of the 200 hPa wind field to AIR.

3. CORRELATION BETWEEN ALL-INDIA RAINFALL AND TROPOSPHERIC TEMPERATURE

We shall now examine the instantaneous and lag correlations of AIR with TT at three spatial scales: the Tibetan Plateau, Eurasian continent and the whole globe.

(a) All-India rainfall and tropospheric temperature over the Tibetan Plateau

The heating over the Tibetan Plateau has been related to the seasonal evolution of the Asian summer monsoon (e.g. Yanai *et al.* 1992). In order to examine the interannual relationship between Indian monsoon rainfall and TT over the Tibetan Plateau, we first calculate the correlation coefficients (CCs) between AIR for the summer monsoon season (June–September, hereafter referred to as JJAS) and the monthly temperature over the Tibetan Plateau (25° – 45°N , 75° – 105°E) at different levels for 1949–98 (Table 1). There are relatively high correlations in spring (March–May, hereafter referred to as MAM) at 200–250 hPa. However, the JJAS AIR exhibits a more significant positive correlation with the plateau air temperature at the levels from 200 hPa to 600 hPa in early autumn (September–October). For example, the 50-year CC between AIR and 250 hPa temperature in September reaches 0.50. However, the correlation becomes negative at 100 hPa although it is still most significant in early autumn. These results show that the monsoon rainfall anomaly leads rather than lags the major temperature variation over the plateau.

The highest correlation between the monthly AIR and monthly temperature appears also around September (Table 2). Taking 200 hPa as an example, we can see that the rainfall–temperature simultaneous CCs are 0.53 and 0.43 in September and October, respectively. The CC between August (September) temperature and September (October) rainfall is 0.30 (0.31), while that between August (September) rainfall and September (October) temperature reaches 0.32 (0.56). Before August there are few significant correlations except those between the March–April temperature and succeeding June rainfall. Also it is noted that the correlation between November AIR and October plateau

TABLE 1. CORRELATION COEFFICIENTS (CCs) OF MONTHLY TROPOSPHERIC TEMPERATURES AT DIFFERENT LEVELS OVER THE TIBETAN PLATEAU (25°–45°N, 75°–105°E) WITH JUNE–SEPTEMBER ALL-INDIA RAINFALL FOR 1949–98

Level	Jan	Feb	Mar	Apr	May	Jun	Jul	Aug	Sep	Oct	Nov	Dec
100 hPa	-0.02	0.08	-0.04	-0.14	-0.07	0.01	-0.06	0.00	<u>-0.46</u>	<u>-0.48</u>	0.03	-0.02
150 hPa	0.13	0.02	0.14	0.05	0.25	0.13	-0.06	0.08	-0.08	0.00	0.04	-0.06
200 hPa	0.17	0.03	0.25	0.22	0.34	0.20	0.09	0.16	<u>0.42</u>	<u>0.44</u>	0.00	0.01
250 hPa	0.20	0.06	0.29	0.22	0.27	0.19	0.13	0.15	<u>0.50</u>	<u>0.42</u>	-0.05	0.01
300 hPa	0.14	0.05	0.16	0.16	0.19	0.16	0.13	0.12	<u>0.49</u>	<u>0.39</u>	-0.09	-0.05
400 hPa	-0.11	0.02	0.04	0.09	0.06	0.10	0.18	0.14	<u>0.47</u>	<u>0.35</u>	-0.09	-0.10
500 hPa	-0.23	0.02	0.01	0.10	-0.01	0.03	0.24	0.16	<u>0.46</u>	<u>0.31</u>	-0.07	-0.11
600 hPa	-0.22	0.06	0.04	0.12	-0.01	0.02	0.28	0.21	<u>0.49</u>	0.25	-0.04	-0.15

The bold numbers and those with underlines denote, respectively, the CCs exceeding the 0.05 and 0.01 significance level.

TABLE 2. CORRELATION COEFFICIENTS BETWEEN THE MONTHLY 200 hPa TEMPERATURE OVER THE TIBETAN PLATEAU AND MONTHLY ALL-INDIA RAINFALL (AIR) FOR 1949–98

Temperature	AIR											
	Jan	Feb	Mar	Apr	May	Jun	Jul	Aug	Sep	Oct	Nov	Dec
Jan	-0.04	0.13	0.24	-0.06	0.12	0.12	0.13	0.17	0.04	-0.03	-0.33	0.14
Feb	0.05	-0.02	-0.03	-0.02	-0.04	0.20	0.00	-0.08	-0.02	-0.05	-0.22	0.16
Mar	-0.03	0.27	0.08	0.08	0.17	0.35	0.07	0.19	0.07	-0.11	-0.01	0.16
Apr	0.01	0.09	-0.04	0.02	0.17	0.29	0.16	0.09	0.04	0.08	-0.108	-0.05
May	0.01	0.13	0.06	-0.32	0.16	0.17	0.27	0.22	0.21	0.08	-0.05	0.03
Jun	0.20	0.20	0.16	-0.16	0.15	0.03	0.15	0.10	0.21	0.21	-0.35	-0.40
Jul	0.13	0.08	0.03	0.10	0.11	-0.08	-0.06	0.11	0.23	0.00	-0.19	-0.01
Aug	0.21	-0.08	0.16	0.02	0.08	-0.12	0.10	0.07	0.30	0.08	-0.19	-0.14
Sep	0.09	-0.16	-0.03	-0.01	0.22	-0.07	0.23	0.32	<u>0.53</u>	0.31	-0.34	-0.27
Oct	-0.08	0.09	-0.03	-0.07	0.24	-0.04	0.23	0.25	<u>0.56</u>	0.43	-0.57	-0.32
Nov	0.01	0.17	-0.12	-0.13	0.24	-0.19	-0.10	0.04	0.22	0.02	0.13	-0.20
Dec	0.08	0.21	-0.03	-0.03	-0.14	0.07	-0.21	0.15	0.03	0.05	-0.28	-0.20

The meaning of the bold and underlined numbers is the same as in Table 1.

temperature is negative and strong. These results show that although there are high correlations between AIR and TT over the Tibetan Plateau their cause–effect relationship is not immediately evident. A possible scenario is that the major increase in the upper TT over the Tibetan Plateau occurs at the end of the monsoon season (September) due to the release of the latent heat of condensation of the monsoon rainfall; the warming in the upper troposphere, in turn, facilitates the maintenance of the land–sea thermal contrast in the post-monsoon month (October) and delays the retreat of the monsoon.

(b) *All-India rainfall and tropospheric temperature over Eurasia*

Some previous analyses have shown the difference in TT over Eurasia between strong and weak Asian summer monsoon years (e.g. Li and Yanai 1996; Kawamura 1998). Considering the possible importance of variations in the TT which could be related to the land surface heating of the Eurasian continent in modulating the Asian monsoon variability, we perform further correlation analyses using data from 50 years. Besides JJAS AIR, a monsoon index (Webster and Yang 1992) defined by the zonal wind shear between 850 hPa and 200 hPa over southern Asia (0°–20°N, 40°–110°E) is calculated for JJAS of each year to reflect the large-scale Asian monsoon intensity. In fact, the CC between JJAS AIR and the monsoon index is as high as 0.52 over 50 years. Meanwhile, the land surface temperature anomaly of the Eurasian continent (20°–60°N,

TABLE 3. CORRELATION COEFFICIENTS (CCs) OF SPRING (MARCH-MAY, MAM) AND SUMMER (JUNE-SEPTEMBER, JJAS) TROPOSPHERIC TEMPERATURE (TT) WITH JJAS ALL-INDIA RAINFALL (AIR), MONSOON INDEX AND EURASIAN LAND SURFACE TEMPERATURE FOR 1949-98

Months	Level (hPa)	CCs of TT with			
		AIR JJAS	Monsoon index JJAS	Land surface temperature MAM JJAS	
MAM	100	-0.19	-0.10	-0.11	0.14
	150	0.06	0.07	0.05	0.00
	200	0.30	0.40	-0.25	-0.08
	250	0.33	0.54	-0.35	0.00
	300	0.29	0.54	-0.24	0.10
	400	0.29	0.50	0.01	0.18
	500	0.30	0.43	0.17	0.28
	600	0.30	0.29	0.47	0.40
	700	0.32	0.30	0.51	0.41
JJAS	850	0.22	0.13	0.69	0.50
	100	-0.27	-0.08	-0.19	0.00
	150	-0.04	-0.03	0.18	0.06
	200	0.40	0.47	-0.04	0.15
	250	0.44	0.57	-0.20	0.22
	300	0.42	0.58	-0.21	0.30
	400	0.45	0.58	-0.15	0.42
	500	0.42	0.55	-0.16	0.45
	600	0.37	0.46	-0.07	0.57
700	0.33	0.44	-0.14	0.57	
850	0.15	0.25	-0.05	0.68	

The bold numbers are the CCs exceeding the 0.05 significance level.

20°-140°E) is extracted from the observational dataset of the University of East Anglia for both the monsoonal summer (JJAS) and the preceding spring (MAM) of every year.

Thus we obtain the CCs of the above four time series with TT averaged for the Eurasian continent (only for land points in (20°-60°N, 20°-140°E)) at various levels in MAM and JJAS (Table 3). Several interesting results can be seen from these CCs. First, for both JJAS AIR and the monsoon index, the CCs with temperature in the upper troposphere are generally larger than those in the lower troposphere. On the other hand, the simultaneous CCs of Eurasian land surface temperature with TT for both MAM and JJAS always decrease with height. These findings suggest that the association between the monsoon rainfall and the upper TT is rather independent from the change in the surface temperature related to land surface processes. Second, the significant correlations between MAM TT and JJAS AIR and the monsoon index show that there is a precursory signal in the Eurasian TT useful for predicting the Indian monsoon rainfall. However, the simultaneous CCs of JJAS TT with JJAS AIR and the monsoon index are generally higher than those of MAM TT. This shows the existence of an instantaneous and strong interaction between the monsoon rainfall and TT over Eurasia. Third, in comparison with AIR, the monsoon index has more significant correlation with TT. For example, the CCs of the monsoon index with 300 hPa temperature in MAM and JJAS, respectively, reach 0.54 and 0.58 while the corresponding CCs of AIR are 0.29 and 0.42. This means that the Eurasian TT under consideration is more strongly associated with the broad-scale monsoon circulation than the regional monsoonal rainfall over the Indian subcontinent.

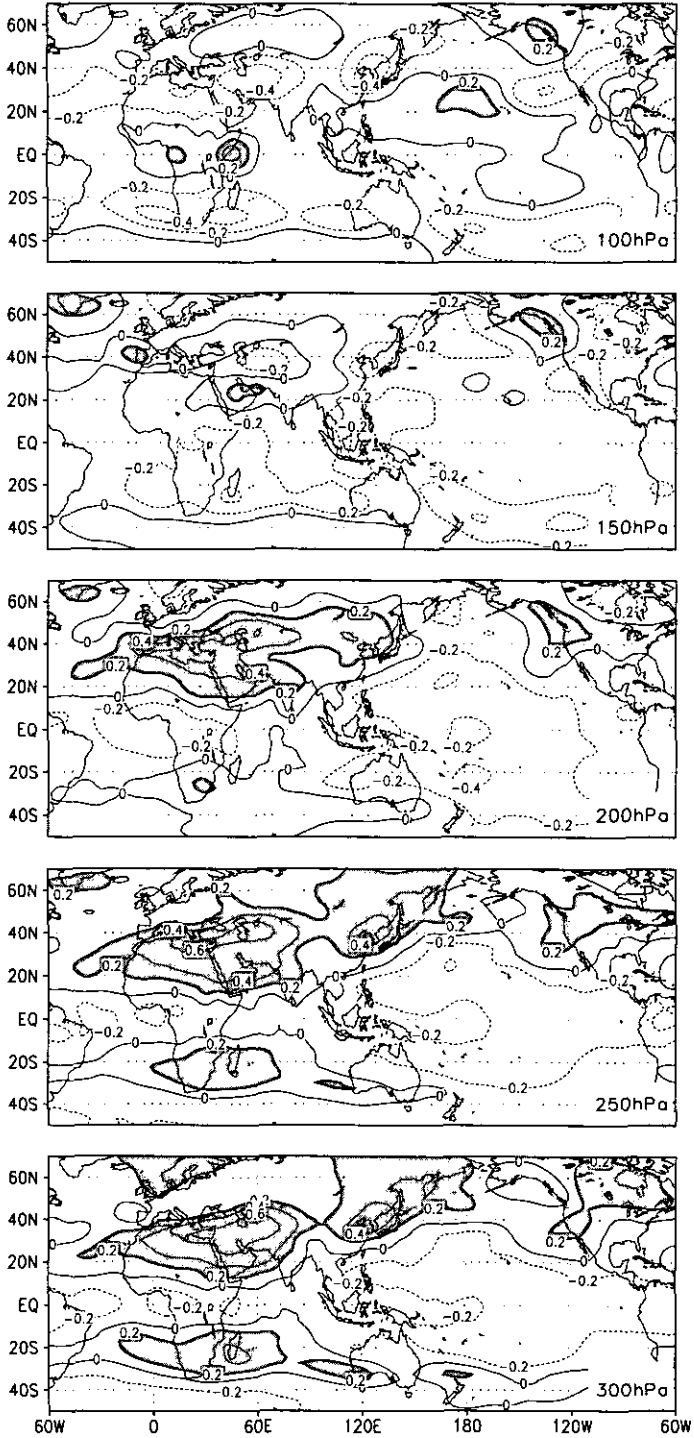


Figure 1. Distributions of correlation coefficients (CCs) between June–September (JJAS) all-India rainfall and JJAS tropospheric temperature at 10 levels from 100 hPa to 850 hPa for 1949–98. The areas with CCs higher than 0.2 are shaded.

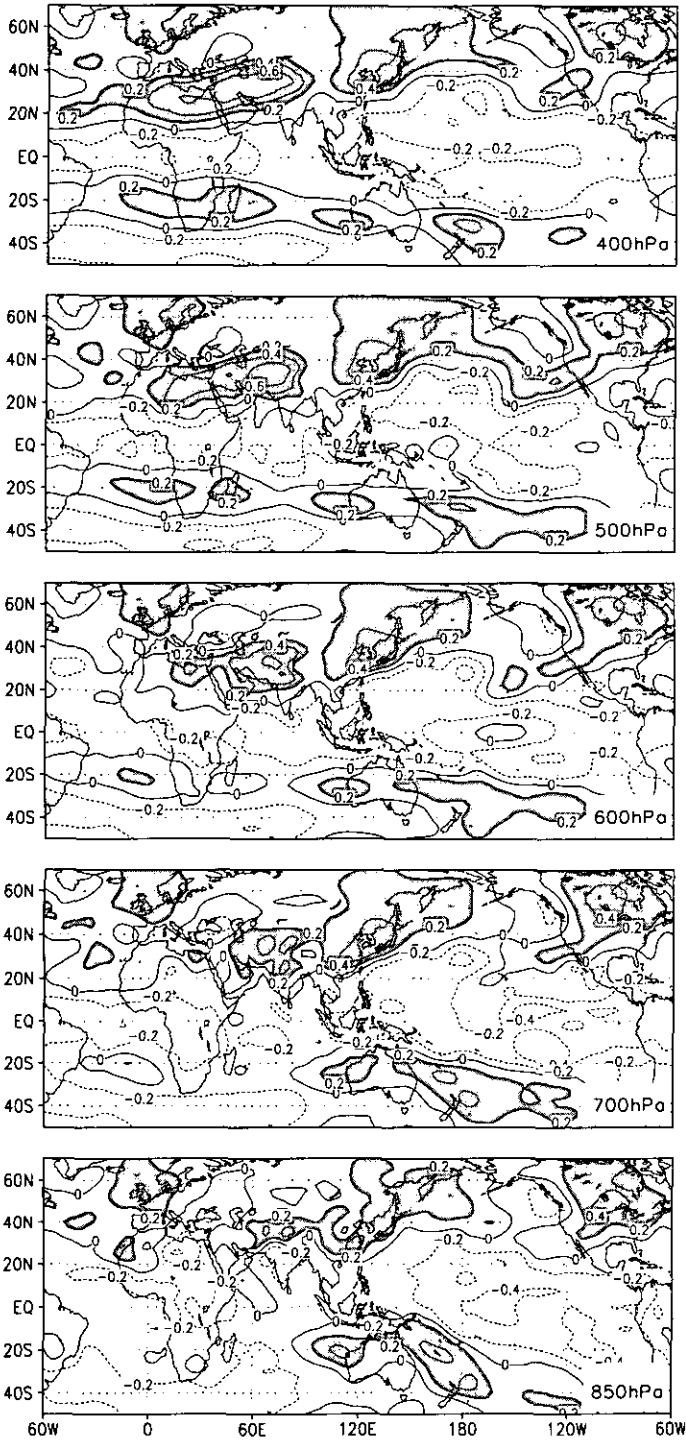


Figure 1. Continued.

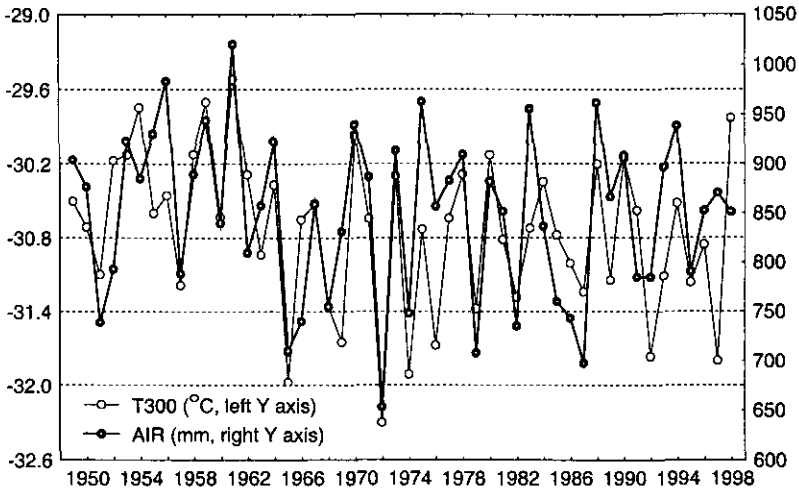


Figure 2. Year-to-year variations of June–September (JJAS) all-India rainfall (AIR) and JJAS 300 hPa temperature (T300) averaged for western Eurasia (20° – 40° N, 10° – 80° E).

(c) *All-India rainfall and global tropospheric temperature*

(i) *Simultaneous correlation.* In fact, the area of high correlation between TT and the Indian monsoon rainfall is not limited to the Tibetan Plateau or Eurasian continent. In Fig. 1 we show the horizontal distributions of CCs between JJAS AIR and JJAS mean temperatures at 100–850 hPa for 1949–98. The correlation patterns in the upper troposphere are more organized than those in the lower troposphere. On the other hand, the CCs in the lower stratosphere (100–150 hPa) show almost opposite signs to those in the upper troposphere. In the upper troposphere from 200 hPa to 400 hPa, there are broad bands with consistently high positive CCs (>0.2) covering large parts of the Eurasian continent and northern Africa. The largest positive CCs are located over the Iran–Mediterranean region rather than the Tibetan Plateau. There are also high positive CCs over East Asia. Meanwhile, in the southern-hemisphere subtropics between about 15° and 30° S, including southern Africa, there exists a band of positive correlation, which is nearly symmetric relative to the equator with its counterpart in the northern hemisphere. Additionally, from the west to the east the bands of high CCs in both hemispheres tend to deflect from the equator. The largest positive correlation in the northern hemisphere occurs over Afghanistan west of the Tibetan Plateau in the middle troposphere (500–600 hPa) and near the east coast of Asia in the lower troposphere (700–850 hPa). There is a tendency for the largest correlations of TT with AIR to gradually shift toward the west from low to high levels.

In view of the high correlation between the monsoon rainfall and upper TT, we calculate yearly JJAS temperatures at 300 hPa averaged for western Eurasia (20° – 40° N, 10° – 80° E) and find that they are highly correlated with the yearly JJAS AIR (Fig. 2), with a CC of 0.68 over 50 years. 1961 (1972) was the wettest (driest) monsoon year over India, corresponding to the highest (lowest) regional average temperature for the past 50 years. It is also noted that there is poor correspondence between the 300 hPa temperature and AIR in El Niño years such as 1966, 1969, 1983, 1992 and 1997. In the following analysis we mainly focus on the 300 hPa temperature which is highly correlated with AIR and its correlation pattern is representative of the upper troposphere.

Figure 3 shows the distributions of simultaneous CCs between the monthly AIR and monthly temperature at 300 hPa from April to November for 1949–98. Here, to save space, only the domain between 40°S and 50°N from 30°W to 150°E is shown because major high correlations are found within this domain, although the CCs are calculated globally. High positive correlations are seen in an extensive area from northern Africa to western Asia, while a zone of positive correlations appears in the southern hemisphere subtropics symmetrically with respect to the equator during July–October, most clearly in September. However, there is no such zone in pre-monsoon (April–May) and post-monsoon (November) months, although an area of positive correlation centred on the Arabian Sea can still be seen in these months. Even in early monsoon (June) when the area of positive correlation extends from northern Africa to western Asia, there is no zone of positive correlation in the southern hemisphere. This suggests that the appearance of two ‘equator-symmetric’ zones of positive correlation far from the equator occur only during, or just after, a mature monsoon.

(ii) *Lag correlation.* In order to examine the lag correlation between AIR and TT, we first calculate the CCs of JJAS AIR and monthly temperatures at 300 hPa (Fig. 4). It is found that the pattern is nearly symmetric with respect to the equator and is most evident in the fields of correlation with temperature in August and September. This pattern also exists in July and October but is absent in other months. The appearance of the symmetric correlation pattern is likely to be related to the existence of the monsoon rainfall. It is also recognized that stronger monsoon rainfall is often associated with the regional warming in the upper troposphere in May over the Arabian Sea and its neighbourhood. The findings of Singh and Chattopadhyay (1998) using observations from a few Indian stations are consistent with the current result obtained by using global and long-term data.

We next calculate the CCs of JJAS AIR with MAM TT at 10 levels to observe whether the springtime TT can be used as a precursory signal for the following Indian monsoon rainfall anomaly. The result (Fig. 5) shows that there are wide regions of high CCs with the maximum values of more than 0.4 over India and the neighbourhood from 200 hPa to 850 hPa, although the regions in the lower troposphere are much narrower than those in the upper troposphere. Using 13-year NCEP/NCAR data, Krishnan and Mujumdar (1999) also found the spring temperature signals and their nearly barotropic structure in the vertical. It can also be seen in Fig. 5 that from 200 hPa to 600 hPa there exist two bands of high positive correlation which are nearly symmetric with respect to the equator. The equator-symmetric patterns are similar to but different from those of the simultaneous JJAS correlation fields (Fig. 1). First, the centres of correlation in Fig. 1 are generally located toward the north and the west compared with those in Fig. 5. Second, the values at the correlation centres in Fig. 1 are much larger than those in Fig. 5. For example, the maximum CC at 250 hPa in the northern hemisphere is 0.56 and located at 20°N over India in Fig. 5, but it is 0.70 and located at 40°N near the Caspian Sea in Fig. 1. From the analysis of Fig. 3 and Fig. 4, we infer that the equator-symmetric patterns appearing in Fig. 1 are related to the existence of the monsoon rainfall. Similarly, we speculate that the equator-symmetric patterns in the fields of correlation between MAM TT and JJAS AIR (Fig. 5) may have actually been the origin of springtime (MAM) rainfall, which is associated with the intertropical convergence zone (ITCZ) rather than the monsoon. From spring to summer, the rainfall increases and moves toward the north because of the onset of the monsoon, therefore the band with positive correlation in the northern hemisphere is enhanced and shifts northwards. The high-correlation band also shifts westwards due to the occurrence of

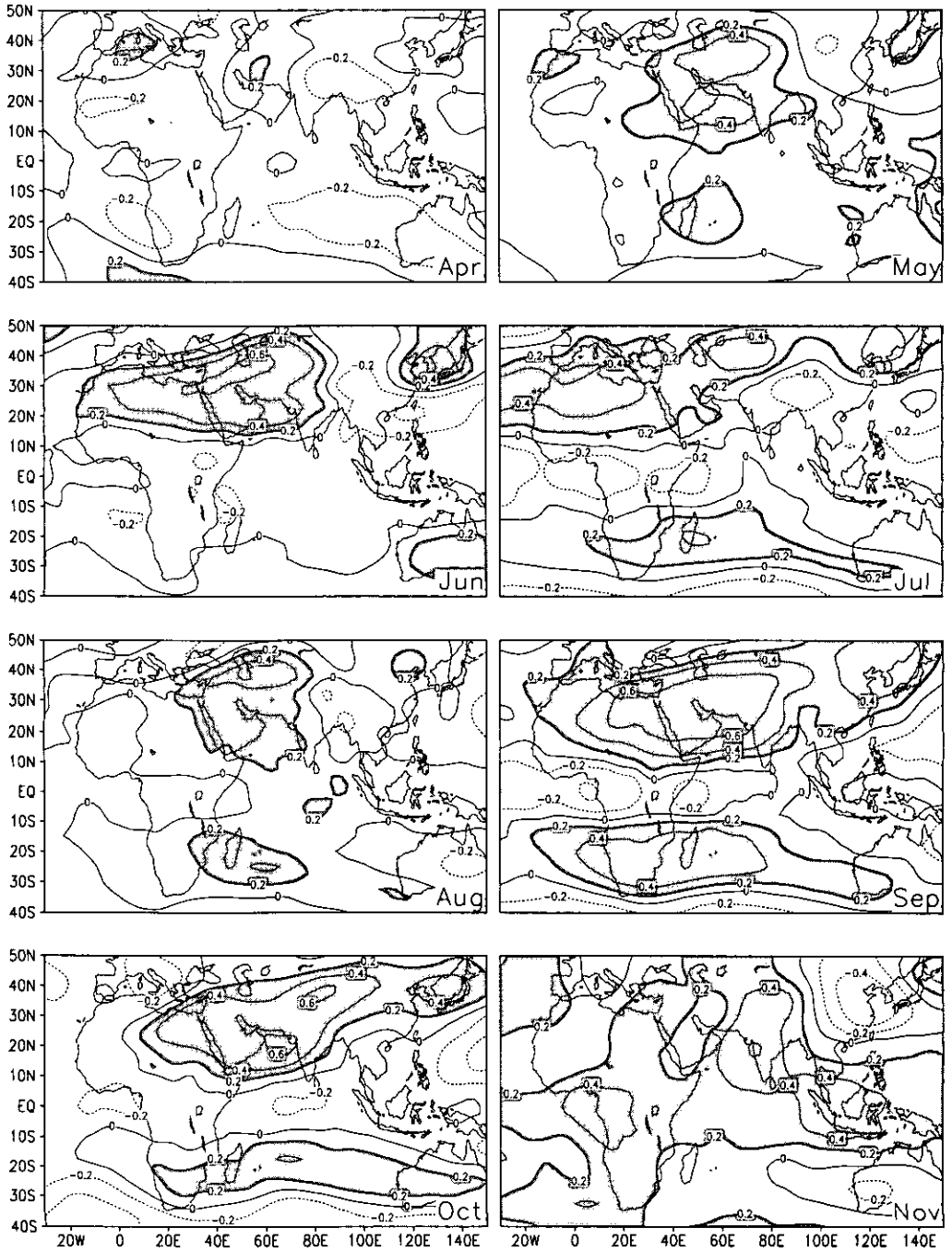


Figure 3. Correlation coefficients (CCs) of monthly 300 hPa temperature from April to November with simultaneous monthly all-India rainfall for 1949-98. The areas with CCs higher than 0.2 are shaded.

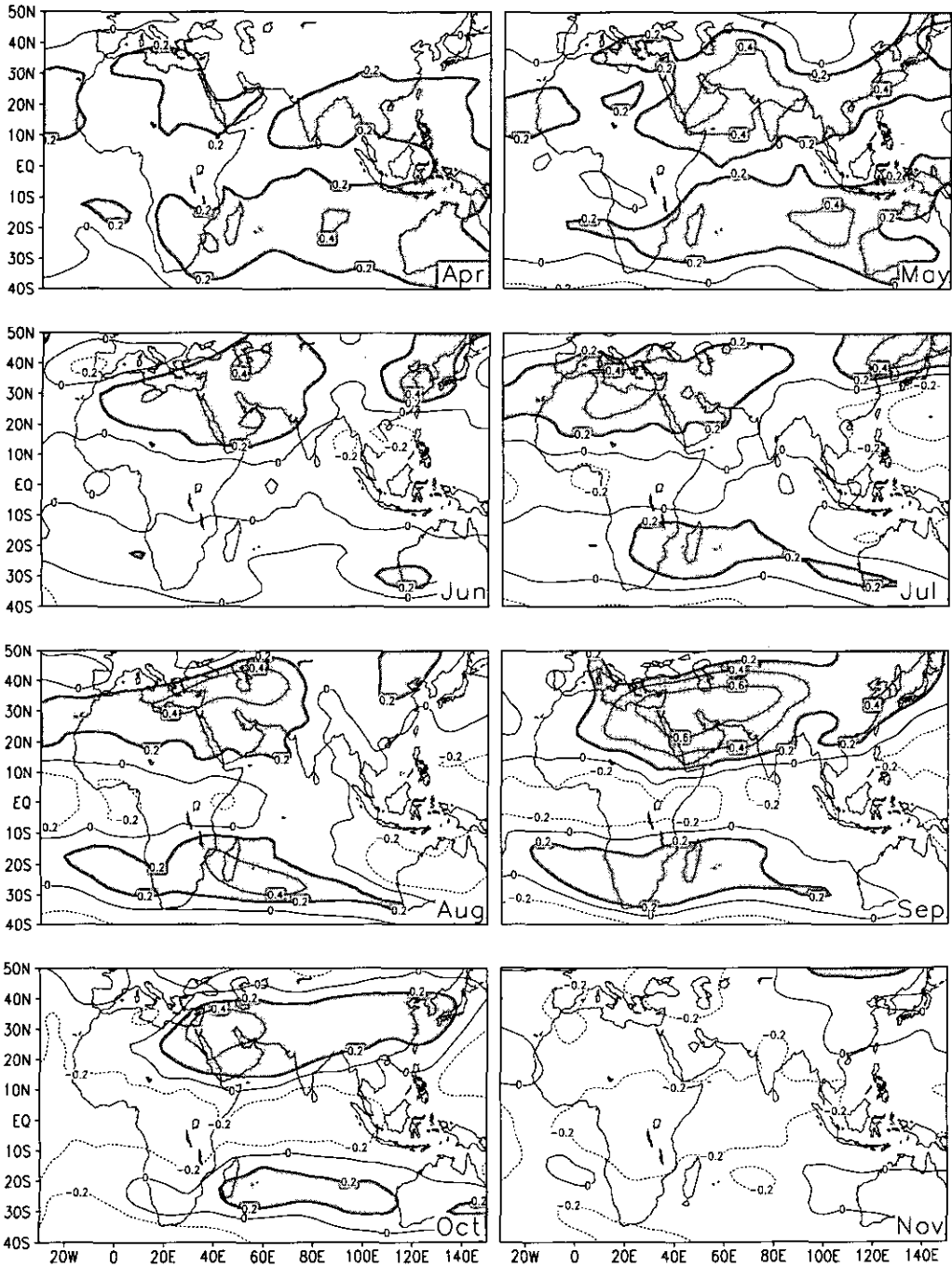


Figure 4. Same as Fig. 3 but with June–September all-India rainfall.

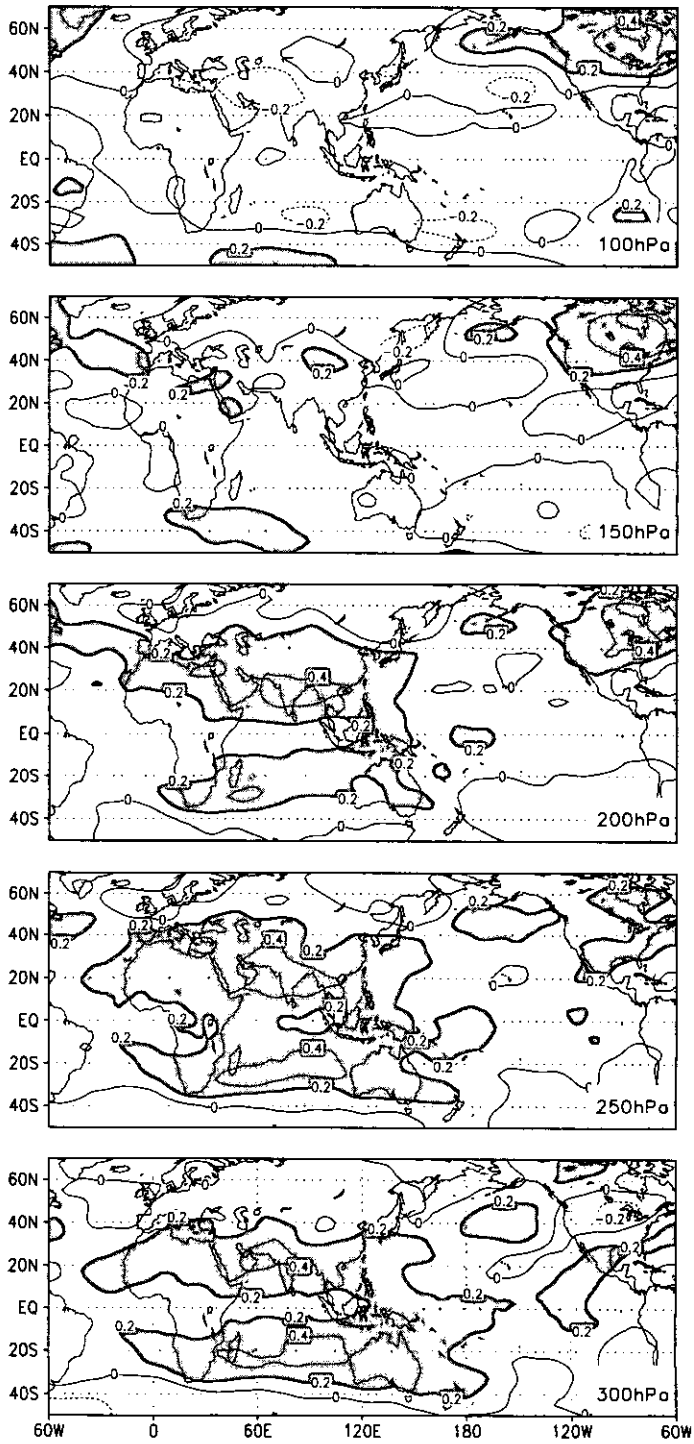


Figure 5. Same as Fig. 1 but for correlation coefficients between June–September all-India rainfall and March–May tropospheric temperature.

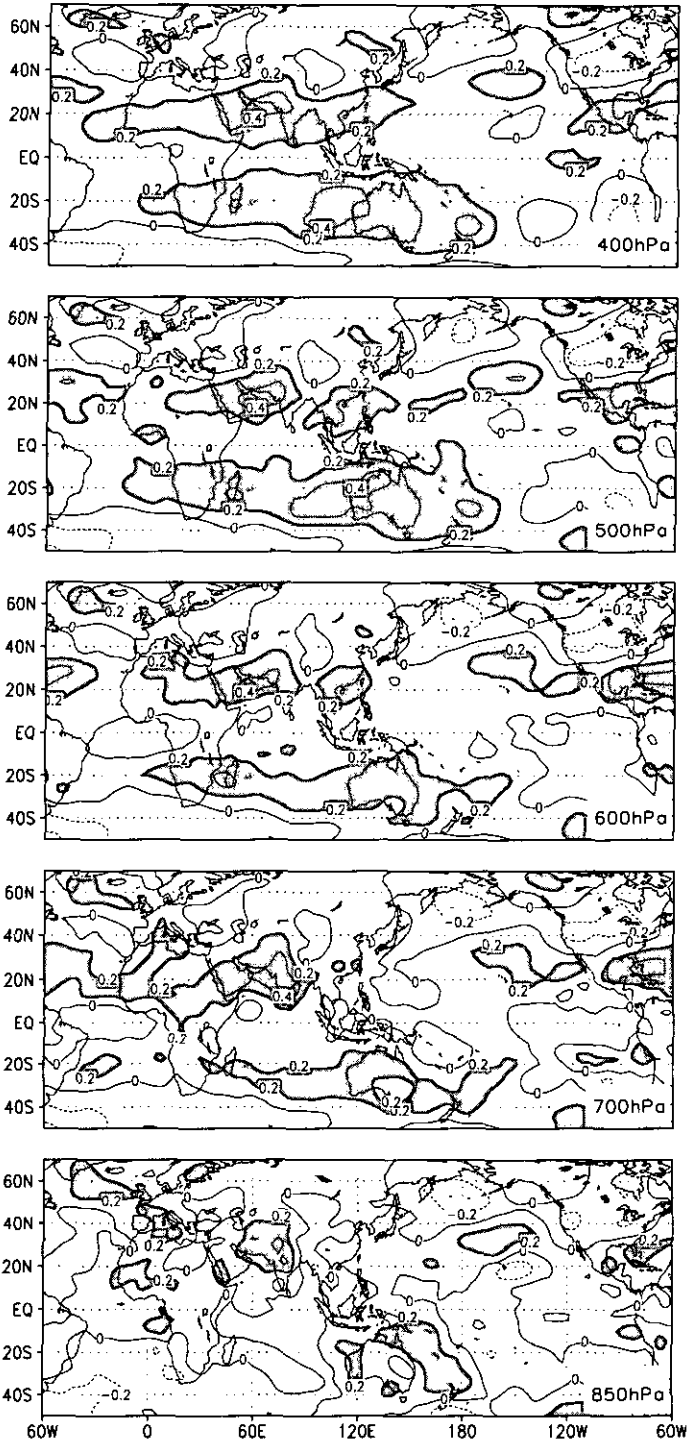


Figure 5. Continued.

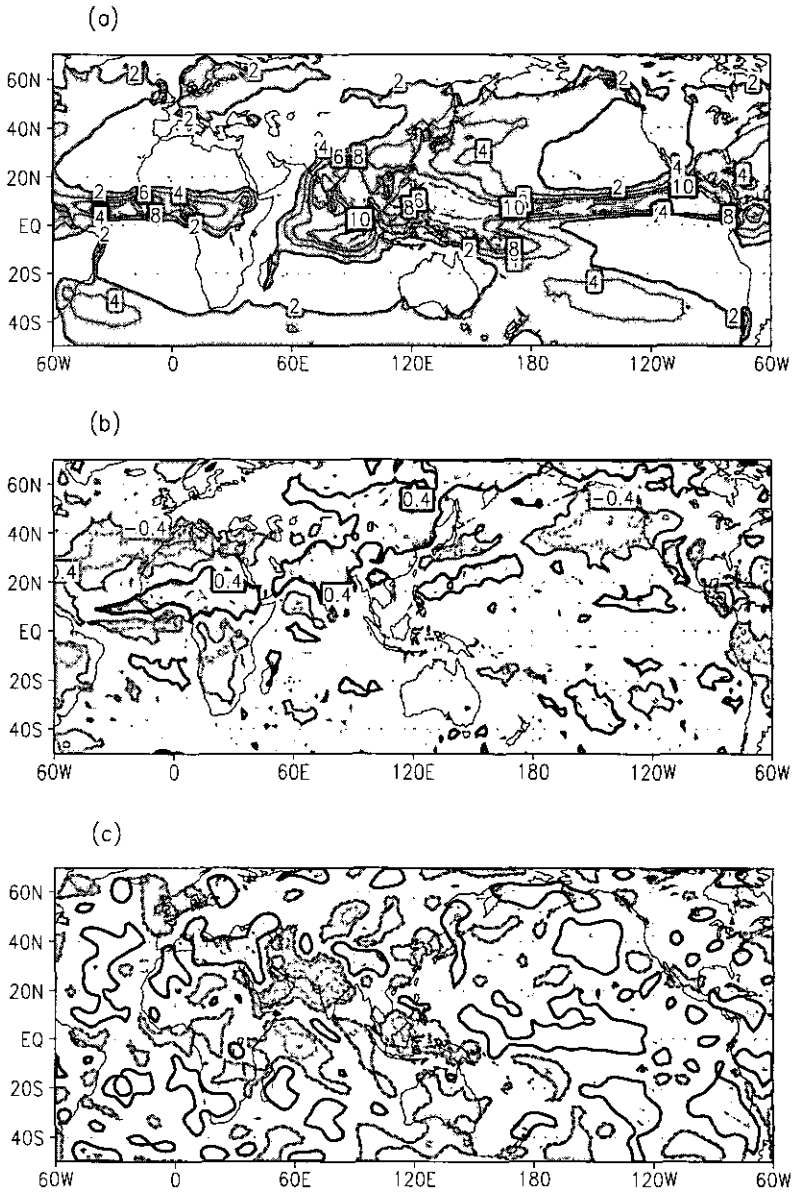


Figure 6. (a) Distribution of the rainfall rate averaged for June–September (JJAS) from 1979 to 1998 (mm day^{-1}); (b) correlation coefficients (CCs) of the monthly rainfall anomalies on the $2.5^\circ \times 2.5^\circ$ mesh with monthly all-India rainfall (AIR) anomalies for 80 summer months (JJAS) from 1979–98. The light and dark shaded areas indicate values less than -0.2 and more than 0.2 , respectively. Only contours of -0.4 , 0.4 and 0.6 are shown; (c) same as (b) but for CCs between 500 hPa vertical pressure velocity and AIR anomalies. The light and dark shaded areas indicate the values less than -0.1 and more than 0.1 , respectively. Only contours of -0.5 , -0.3 , -0.1 , 0.1 and 0.3 are shown.

the African monsoon rainfall (Fig. 6(b)). Thus, it is more likely that the MAM TT anomaly over India results from the anomaly in MAM tropical rainfall rather than that in the land surface processes. Once established, the MAM TT anomaly may lead to the establishment of anomalies in the land-sea temperature gradient and the corresponding monsoon rainfall in summer. More discussion on the role of land surface processes in the monsoon rainfall variability is given in section 5.

4. COUPLING BETWEEN THE MONSOON RAINFALL AND UPPER-TROPOSPHERIC TEMPERATURE ANOMALIES

We have shown that a strong correlation exists between the JJAS temperature in the upper troposphere and the JJAS AIR. In this section, we focus our attention on the coupling between the upper TT and instantaneous monsoon rainfall anomalies. From the JJAS average global rainfall distribution for the most recent 20 years (Fig. 6(a)), we can recognize two main rain belts, i.e. a broad zone over the Indian Ocean-western Pacific warm pool, the other from Africa to the eastern Atlantic between about 15°N and the equator. These two zones are connected by the ITCZ rain belts of the Pacific and Atlantic. The dry desert region extending from north Africa to western Eurasia has been explained with different mechanisms by Charney (1975), Broccoli and Manabe (1992) and Rodwell and Hoskins (1996). The distribution of the CCs between the monthly AIR anomalies and monthly rainfall anomalies at every grid point of the $2.5^\circ \times 2.5^\circ$ mesh (Fig. 6(b)) for 80 summer months (JJAS of 1979-98) shows that AIR anomalies are positively correlated with the rainfall anomalies over northern tropical Africa and those over East Asia (especially North China). We also note that the rainfall anomalies in the 'dry' region such as the North Atlantic-Mediterranean Sea, western Eurasia and southern Africa and eastern North Pacific are negatively correlated with the Indian monsoonal rainfall, suggesting the effect of large-scale subsidence enhanced by the intensified Hadley circulation.

In a multi-year JJAS average distribution of the 500 hPa vertical velocity (not shown), one can observe that strong ascending motion is mainly concentrated in the Bay of Bengal, western Pacific warm pool and northern tropical Africa, while subsidence occurs near the Mediterranean Sea, southern Indian Ocean and eastern Pacific. The above distribution of vertical motion corresponds well with the pattern of mean summer rainfall and dry regions (Fig. 6(a)). From the correlation between the monthly 500 hPa vertical pressure velocity and instantaneous AIR anomalies for 80 summer months during 1979-98 (Fig. 6(c)), it is clearly seen that the ascending motion generally strengthens from southern Asia to tropical Africa with the increase in AIR. At the same time, the descending motion is intensified over eastern Mediterranean, southern Africa and equatorial eastern Pacific, probably due to enhanced local Hadley and Walker circulations linked to the Asian-African monsoon rainfall anomaly.

Because the rainfall amounts over East Asia are relatively small (Fig. 6(a)), we consider that simultaneous variations in the rainfall (and thus in released latent heat of condensation) from tropical Africa to the Indian Ocean may have a major impact upon the atmospheric variability. In the following SVD analysis, we use OLR as a proxy for rainfall because of technical difficulties in normalizing the rainfall data which have a highly skewed distribution. We apply the SVD analysis to the OLR data in an area including tropical Africa and India (Fig. 7(a)) and temperature at 300 hPa to explore their coupled relationship. The area of the 300 hPa temperature field for SVD analysis (Fig. 7(b)) is chosen according to the correlation pattern of the temperature with AIR (see Figs. 1, 3 and 4). In Fig. 7(a), regions of low OLR values that represent strong

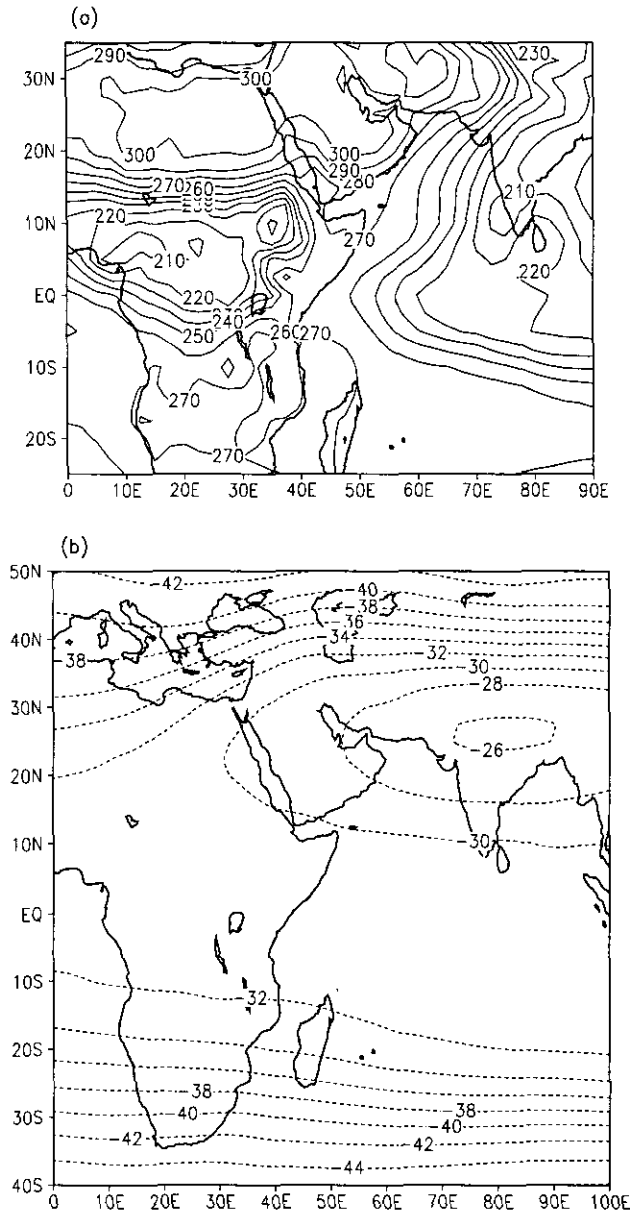


Figure 7. 1979-98 June-September average fields of (a) outgoing long-wave radiation (W m^{-2}) and (b) temperature at 300 hPa ($^{\circ}\text{C}$).

convective activities are located in tropical Africa and the Indian Ocean. In the 300 hPa temperature field (Fig. 7(b)), there is a warm centre to the south of the western Tibetan Plateau. After normalizing the monthly OLR and 300 hPa temperature anomalies, we perform the SVD calculation using the data for a total of 80 sample months of JJAS for 1979-98.

A summary of the statistics for the SVD analysis is shown in Table 4, in which the squared covariance fraction (SCF), the cumulative squared covariance fraction (CSCF)

TABLE 4. SUMMARY OF THE SINGULAR VALUE DECOMPOSITION (SVD) ANALYSIS FOR OUTGOING LONG-WAVE RADIATION AND 300 HPA TEMPERATURE ANOMALY FIELDS

SVD mode	SCF (%)	CSCF (%)	CC
1	48.8	48.80	0.67
2	14.75	63.55	0.59
3	7.7	71.25	0.77
4	6.39	77.64	0.58
5	4.25	81.89	0.72

SCF = squared covariance fraction, CSCF = cumulative squared covariance fraction, and CC = correlation coefficient.

and the CC between the time coefficients of the SVD mode in the two fields are listed. The SCF indicates the percentage of the total squared covariance explained by the SVD mode and is a measure of the relative importance of that SVD mode in the relationship between the two fields. The SCF of the first SVD mode reaches 48.8%, and the corresponding CC is 0.67. Such a large SCF value implies that this coupled mode reflects nearly a half of the linear interaction between the rainfall and upper TT anomalies in summer monsoon months. The SCF and CC for the second SVD mode are 14.75% and 0.59, respectively, while the SCFs for other modes are all below 10%. The CSCF from the first two SVD modes explains 63.55% of the total squared covariance and they are the most important leading modes. For this reason we concentrate our analysis on the first two SVD modes.

Figure 8 shows the so-called heterogeneous correlation patterns of the first SVD mode for both OLR and temperature. The heterogeneous correlation pattern means the correlation pattern of the time coefficient of a mode in one field with the other field. It shows how the two fields are related to one another. The spatial pattern of OLR associated with the first SVD mode is dominated by a broad region of negative correlation from tropical Africa to India (Fig. 8(a)), corresponding to simultaneous variations of rainfall in these areas (see Fig. 6(b)). Coupled with this OLR pattern, the temperature pattern (Fig. 8(b)) for the first SVD mode shows a distribution symmetric with respect to the equator, with high positive values over subtropical areas in both hemispheres and negative values along the equator covering Africa. This pair of coupled patterns indicates that when the monsoon from tropical Africa to India becomes more intense (i.e. the OLR anomaly is negative), the upper troposphere becomes warmer over the areas from northern Africa to western Asia and in the southern-hemispheric subtropics covering southern Africa.

The second pair of coupled patterns also reflects the association of the rainfall or convection heating anomaly in the Asian-African monsoon with the warming in the upper troposphere over the mid latitudes of the Eurasian continent. The spatial patterns of the second SVD mode are shown in Fig. 9. The heterogeneous correlation field of OLR (Fig. 9(a)) links negative anomalies from western Africa to Saudi Arabia, and positive anomalies in India, the Indian Ocean and southern Africa. Meanwhile, the heterogeneous correlation map of temperature (Fig. 9(b)) also represents an equator-symmetric pattern, but the equatorial zone of negative values becomes broader and the areas of positive values are shifted towards higher latitudes compared with the corresponding areas for the first SVD mode (see Fig. 8(b)).

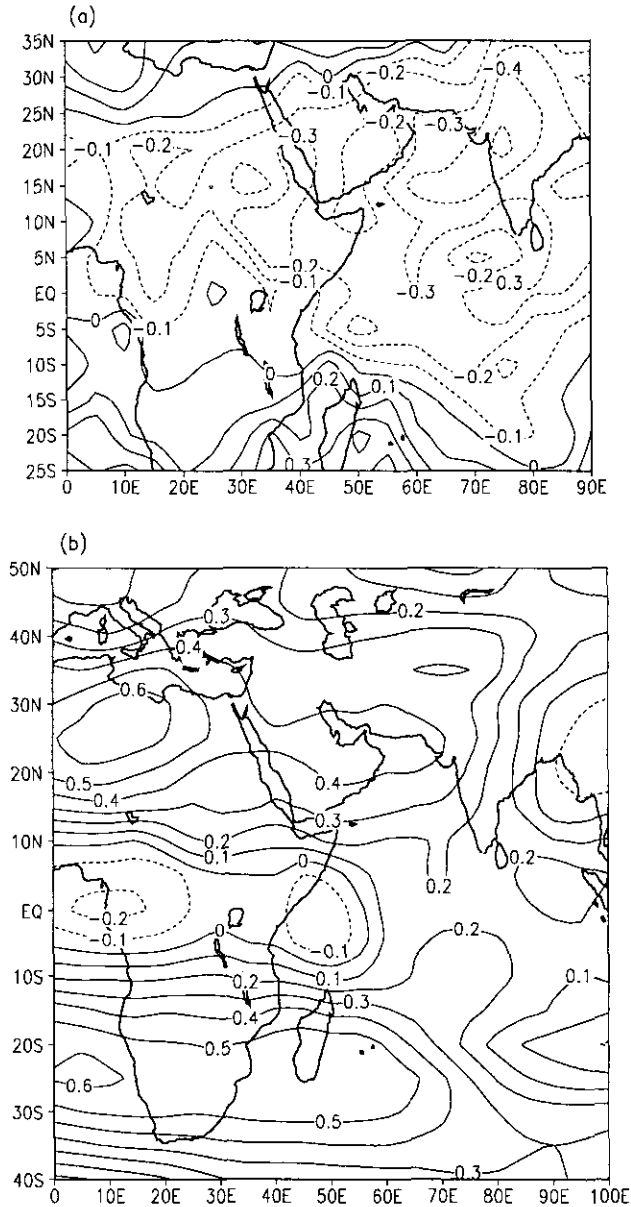


Figure 8. Heterogeneous correlation patterns of the first singular value decomposition mode for (a) outgoing long-wave radiation and (b) 300 hPa temperature.

Because the first SVD mode for OLR is the leading mode which reflects the coherent variation in the Asian–African monsoon rainfall, we calculate the correlation pattern between the time coefficient of the first SVD mode for OLR and temperature anomalies for 80 summer months from 1979 to 1998 (Fig. 10(a)). Prominent characteristics in the correlation field are its symmetry with respect to the equator in the south–north direction and its anti-symmetry with respect to about 85°E in the east–west direction. Interestingly, the correlation pattern is very similar to that between the monthly AIR and temperature anomalies for the same 80 months over 20 years (Fig. 10(b)) as well as

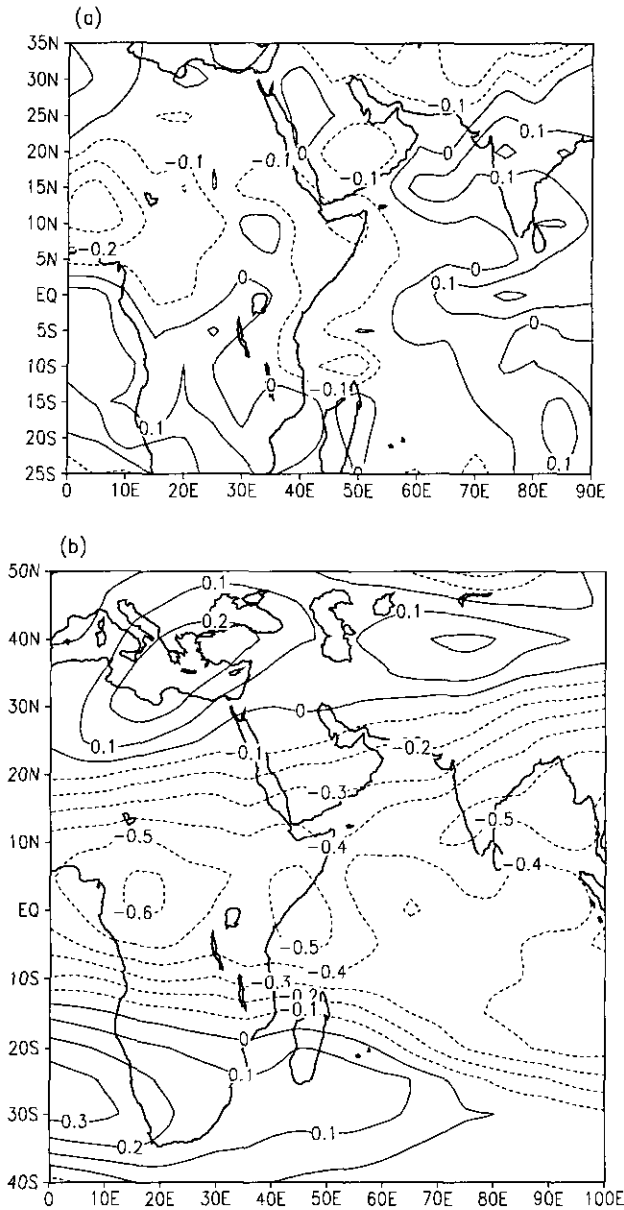


Figure 9. Same as Fig. 8 but for the second singular value decomposition mode.

those for seasonal (Fig. 1) and monthly (Fig. 3) averages over 50 years. The reason for the similarity rests with the high positive correlation between the time coefficient of the first SVD mode for OLR and AIR anomalies (Fig. 11), reaching 0.61 for 80 months and 99.9% confidence level. In other words, the first SVD mode for OLR indeed indicates the coherent rainfall variations in the Asian–African monsoon areas. Thus, it is clear that there exists a closely coupled relation between the monsoon rainfall and upper TT. In the following section, we explore the possible mechanism relating the monsoon rainfall to the upper TT.

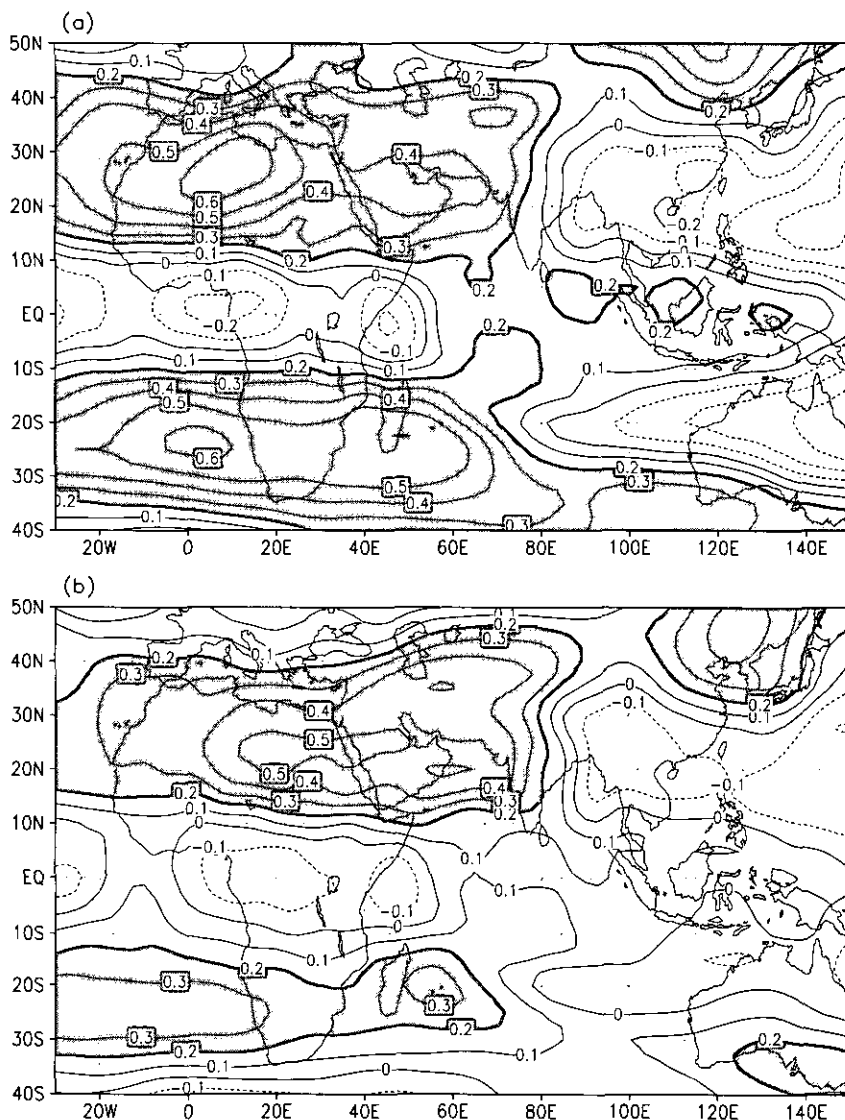


Figure 10. Correlation patterns of 300 hPa temperature anomalies with (a) the time coefficients of the first singular value decomposition mode for outgoing long-wave radiation and (b) all-India rainfall anomalies, for 80 summer months during 1979-98.

5. POSSIBLE MECHANISMS RELATING THE MONSOON RAINFALL TO UPPER-TROPOSPHERIC TEMPERATURE

(a) *Summer temperature and summer rainfall*

There are two possible explanations concerning the observed simultaneous correlation between the monsoon rainfall and upper TT in the subtropics. (1) Both the warming in the upper troposphere and strengthening of the monsoon (i.e. increasing of the monsoon rainfall) are directly induced by the anomalous heating from the land surface of the Eurasian continent. (2) The latent heat of condensation released with the monsoon

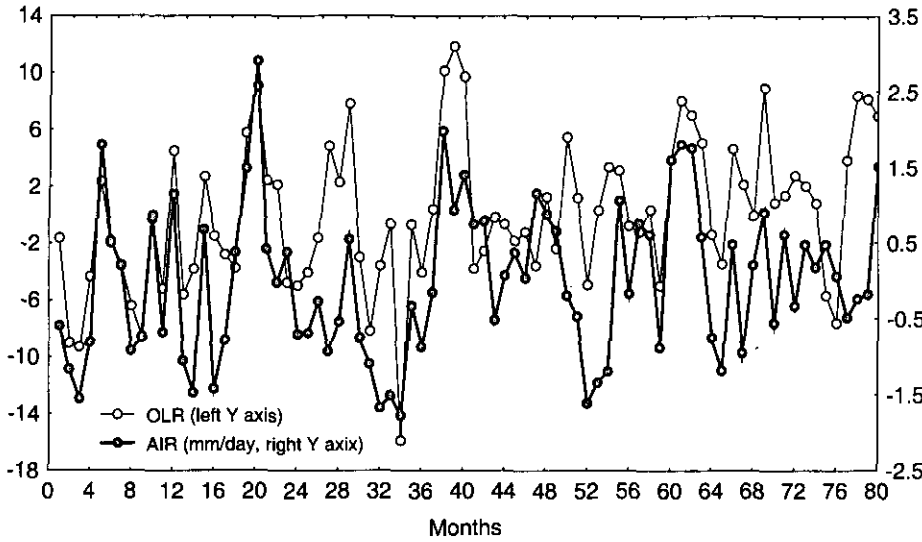


Figure 11. The time coefficients of the first singular value decomposition mode for outgoing long-wave radiation (OLR) and all-India rainfall (AIR) anomalies for 80 summer months during 1979-98.

TABLE 5. CORRELATION COEFFICIENTS (CCs) BETWEEN ALL-INDIA RAINFALL (AIR), MONSOON INDEX, EURASIAN LAND SURFACE TEMPERATURE, AND NINO3 SEA SURFACE TEMPERATURE (SST) FOR THE MOST RECENT 50 YEARS

	Land surface temperature		SST	
	MAM	JJAS	MAM	JJAS
AIR	0.14	0.12	-0.17	-0.58
Monsoon index	-0.09	0.02	-0.45	-0.61
	0.41		0.59	

The number 0.41 (0.59) in the last row is the CC between March-May (MAM) and June-September (JJAS) land surface temperature (sea surface temperature). The bold numbers indicate the CCs exceeding the 0.01 significance level.

rainfall may cause the atmospheric circulation anomaly and then result in the warming in the upper troposphere in the subtropics either by subsidence or advection.

To examine the first possibility, we review Table 3. It is interesting to note that the CCs of JJAS AIR or the monsoon index with the JJAS TT averaged for the Eurasian continent in the upper troposphere are larger than those in the lower troposphere. For example, the CCs of JJAS AIR with the JJAS TT at 250 hPa and 850 hPa are 0.44 and 0.15, respectively. However, the CCs of JJAS Eurasian land surface temperature with JJAS Eurasian TT in the upper troposphere are smaller than those in the lower troposphere. For example, the CCs of JJAS Eurasian land surface temperature with the JJAS TT at 250 hPa and 850 hPa are 0.22 and 0.68, respectively. These facts suggest that the high correlation between the upper TT and the monsoon rain is not a direct result of the heating from the land surface of the Eurasian continent. From Table 5, we can find that the CCs of JJAS Eurasian land surface temperature with the JJAS AIR and monsoon index are only 0.12 and 0.02, respectively. Such a low correlation also shows weak dependence of the monsoon variability on the land surface temperature.

On the other hand, we have seen evidence that the upper TT variability is caused by the tropical rainfall anomaly related to the monsoon. We noticed that during the summer monsoon season the areas with intensified subsidence (i.e. the areas of positive correlation in Fig. 6(c)) generally correspond to those of upper-tropospheric warming (i.e. the areas of positive correlation in Fig. 10(b)) and drying (i.e. the areas of negative correlation in Fig. 6(b)). This situation suggests that the adiabatic warming related to intensified subsidence is mainly responsible for the warming in the upper troposphere over the eastern Mediterranean and southern Africa. Strong subsidence warming to the west of the major rain area was shown by He *et al.* (1987) and Yanai *et al.* (1992) during the onset of the summer monsoon of 1979.

Figure 12(a) gives the climatological JJAS streamline field at 200 hPa, which shows a strong anticyclonic system centred over the south flank of the Tibetan Plateau, dominant westerly flows north of the anticyclone and easterly flows south of the anticyclone. However, in the anomaly streamline field at 200 hPa regressed with AIR anomaly for 80 summer months from 1979 to 1998 (Fig. 12(b)), two major anticyclonic circulation centres can be seen over Iran–Afghanistan in the northern hemisphere and east of Madagascar in the southern hemisphere. This regression streamline field means that stronger tropical convection heating with the intensified Indian monsoon rainfall facilitates the development of anomalous anticyclonic circulations in the subtropics of both hemispheres. The forced circulation anomaly is similar to a response of stationary Rossby waves to the near-equatorial heat source as discussed by Matsuno (1966), Webster (1972) and Gill (1980). Rodwell and Hoskins (1996) found that the diabatic heating from the Asian monsoon can induce a Rossby-wave pattern to the west by using an idealized model. Ogasawara *et al.* (1999) also found similar atmospheric responses to the tropical convection anomaly related to the Australian monsoon in the northern winter season in a coupled general-circulation model. It is especially noteworthy that anomalous south-westerly flow west of the anticyclonic centres in Fig. 12(b) exists over the regions from northern Africa to central Asia where the upper TT rises when the monsoon rainfall increases (Fig. 10(b)). The warming in the upper troposphere over these regions may partially be a result of the temperature advection by an atmospheric circulation in response to the strong heating anomaly associated with the monsoon rainfall. Similarly, the warming over southern Africa can be related to anomalous north-easterly flow. Consequently, a correlation pattern, symmetric with respect to the equator, of upper TT with the monsoon rainfall is thought to be a manifestation of the atmospheric response to the anomalous tropical heating with the varying monsoon rainfall.

(b) *Spring temperature and summer rainfall*

It is very interesting to know how the springtime temperature is related to the summer monsoon rainfall. It may be recalled that in Table 3 the MAM upper TT over the Eurasian continent exhibits significant correlation with JJAS AIR and the monsoon index. The highest correlation is found near the Indian subcontinent from 200 hPa to 700 hPa (see Fig. 5). However, it is worth noting that the simultaneous CCs of the Eurasian land surface temperature with TT, decrease with height for both MAM and JJAS (Table 3). This suggests that the variation of land surface temperature has an impact on the lower troposphere rather than the upper troposphere where the temperature has a close correlation with the Indian monsoon rainfall. A previous observational study (Sankar-Rao *et al.* 1996) showed that the temperature perturbations induced by the variation in the land surface processes associated with the Eurasian snow-cover anomaly are limited below the 500 hPa level. A number of numerical modelling studies also

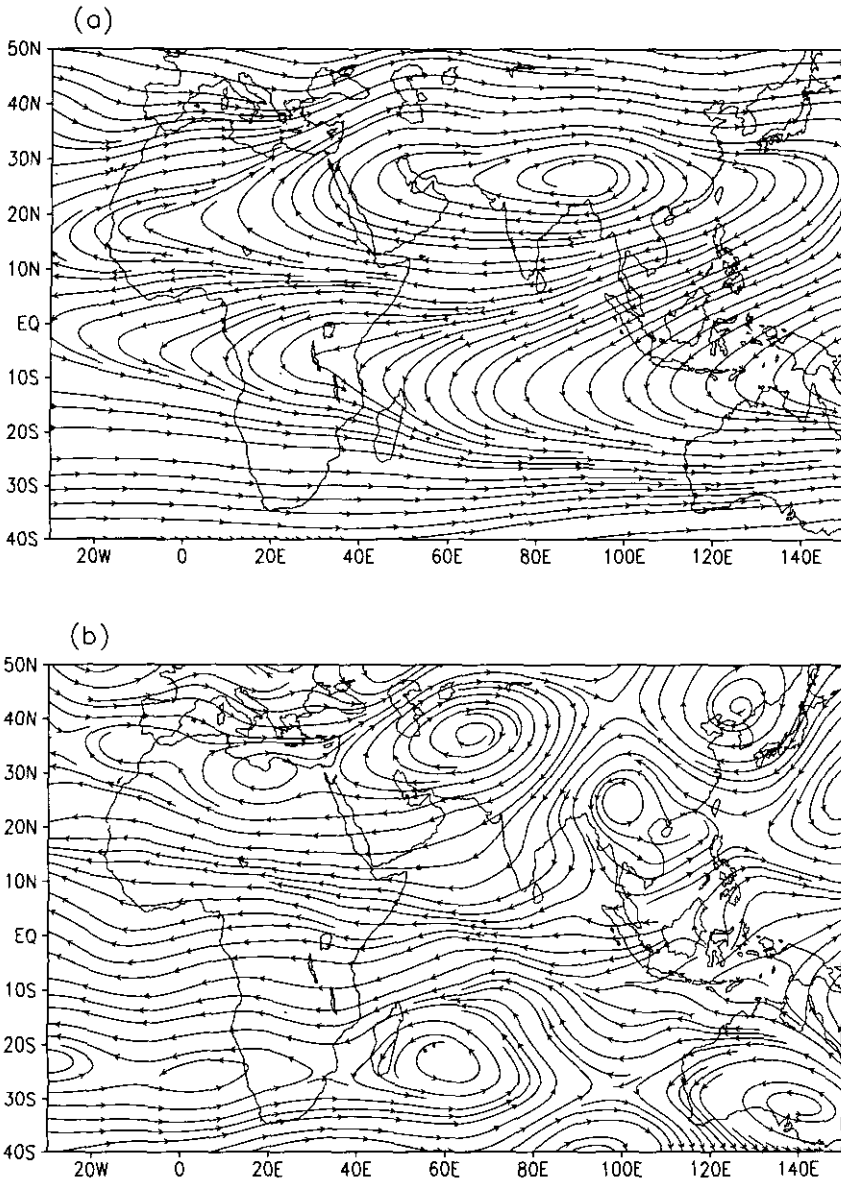


Figure 12. (a) 1979-98 June-September mean streamline field at 200 hPa. (b) The anomaly streamline field at 200 hPa regressed with all-India rainfall anomalies for 80 summer months during 1979-98.

showed that influences of the snow cover (Vernekar *et al.* 1995; Ose 1996) or soil moisture (Fennessy and Shukla 1999) on the air temperature are mainly confined to the lower troposphere. Table 3 also shows that the MAM land surface temperature generally has low, and even negative correlation with JJAS TT, but the MAM lower TT has significant positive correlations with JJAS land surface temperature. This suggests that the spring land surface temperature anomaly does not lead the following summer TT anomaly, while the MAM TT may impact on the JJAS land surface temperature.

In order to further examine the persistence of TT anomalies from spring to summer, the CCs between MAM TT and JJAS TT for each point at 10 levels are calculated

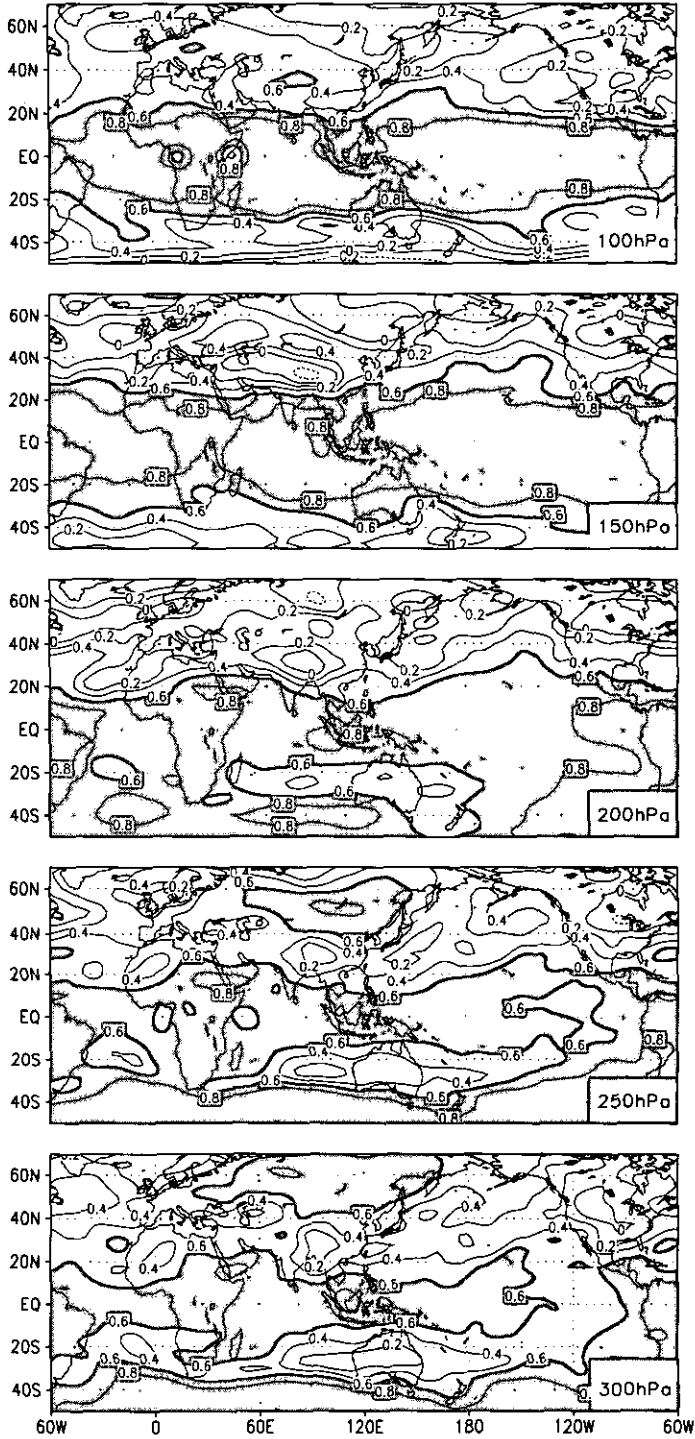


Figure 13. Distributions of correlation coefficients (CCs) between March–May tropospheric temperature (TT) at every point and June–September TT at the same points at 10 levels from 100 hPa to 850 hPa for 1949–98. The areas with CCs higher than 0.6 are shaded.

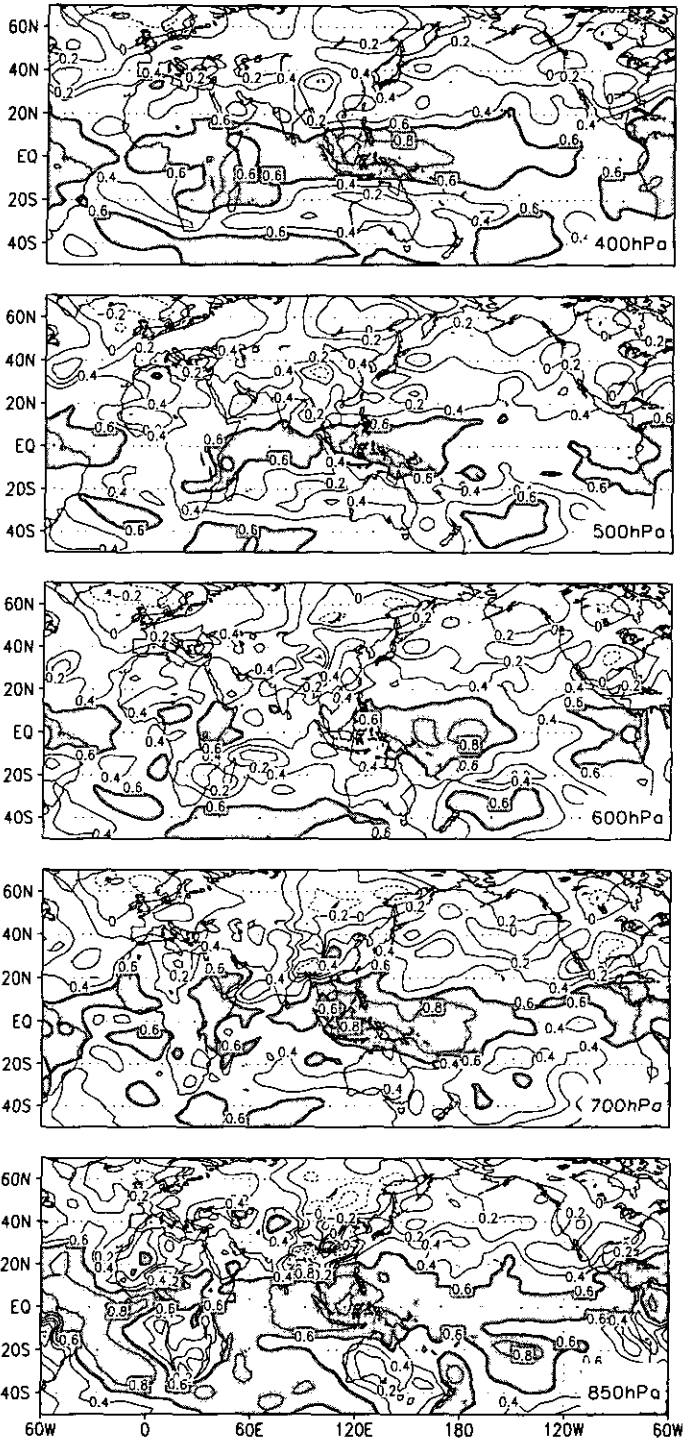


Figure 13. Continued.

(Fig. 13). Several important features are seen in Fig. 13. The correlation is generally larger in the upper troposphere than in the lower troposphere and it is larger in the tropics than in the subtropics. We note that the degree of persistence is low in the lower troposphere over most of Eurasia. However, the persistence is exceptionally strong (where the CCs are above 0.6) at 250 hPa and 300 hPa and over northern Eurasia, compared with other levels or the rest of the mid latitudes. This persistent temperature anomaly in the upper troposphere undoubtedly helps to lead the summer monsoon and its rainfall anomalies. It is not clear, however, why there exists such persistence in the upper TT from spring to summer over northern Eurasia, although it appears that the persistence is not caused by the persistent anomaly in the land surface temperature.

We can further discuss the effect of the surface temperature on the monsoon and its rainfall. As shown in Table 5, the MAM or JJAS Eurasian land surface temperature is found to have very small correlation with JJAS AIR or the monsoon index although the land surface temperature presents evident persistence from spring to summer, the CC being 0.41 between the land surface temperature in MAM and that in JJAS. On the other hand, AIR or the monsoon index represent significant negative correlation with NINO3 SST. For example, the CCs of the JJAS monsoon index with the MAM SST and JJAS SST are -0.45 and -0.61 , respectively. Moreover, the persistence of the SST anomaly is stronger, with a CC of 0.59 between MAM SST and JJAS SST. This means that the variability of the Asian monsoon is controlled more strongly by the SST in the eastern equatorial Pacific than by the Eurasian land surface temperature. The modelling study of Lau and Nath (2000) showed the essential importance of SST anomalies and relative unimportance of the atmosphere–land interactions in determining the monsoon variability. Results of other numerical experiments (Lau and Bua 1998; Yang and Lau 1998) also showed that SST anomalies have a stronger effect on the monsoon variability compared with anomalies in the land surface processes. It is worth exploring whether the SST anomaly in the equatorial Pacific determines the anomaly of spring upper TT (e.g. as shown in the Fig. 11 of Shen *et al.* (1998)), maintains the persistence of temperature in the upper troposphere over Eurasia from spring to summer, and eventually leads to a strong or weak summer monsoon. In short, the springtime temperature anomaly in the upper troposphere over Eurasia, including the Indian subcontinent, may result from the SST and simultaneous tropical rainfall anomalies, while the action of the land surface processes may not be crucial. The springtime TT anomaly, once established, will promote the anomaly of the summer monsoon.

6. CONCLUSION AND DISCUSSION

Based on various observational data, the relationship between the Indian monsoon rainfall and TT on different spatial scales, the Tibetan Plateau, Eurasian continent and the entire globe, is examined using the correlation analysis and SVD analysis methods. The major findings are:

- There exist significant positive correlations between JJAS AIR and 200–600 hPa temperatures averaged for the Tibetan Plateau (25° – 45° N, 75° – 105° E) in September and October. The JJAS AIR and the Asian monsoon index (Webster and Yang 1992) have significant positive correlations with 200–700 hPa temperatures averaged for the Eurasian continent (20° – 60° N, 20° – 140° E) for both MAM and JJAS. The highest lag correlation of JJAS AIR with MAM TT occurs over India and its neighbourhood.
- A band with the highest positive correlation of the JJAS temperature in the upper troposphere with JJAS AIR appears mainly in western Eurasia, i.e. from the southern Mediterranean Sea–northern Africa regions to western and central Asia. There is a band

of positive correlation in the southern hemisphere subtropics covering southern Africa and Madagascar, which is located nearly symmetrically with respect to the equator relative to the northern band. This 'equator-symmetric' correlation pattern disappears in pre-monsoon and post-monsoon seasons.

- The upper TT anomalies are closely coupled with the variations in OLR related to the monsoon rainfall over Asia and Africa in summer. The first SVD mode from the SVD analysis between OLR and 300 hPa temperature explains 48.8% of the total squared covariance and the CC between the time coefficients of the first SVD mode in the two fields reaches 0.67. The spatial pattern of OLR associated with the first SVD mode indicates the coherent variations in convective activity related to the rainfall from tropical Africa to India, while the temperature pattern for the first SVD mode has a structure which is symmetric with respect to the equator, with consistent anomalous values from northern Africa to western Asia and over the southern-hemispheric subtropics, and anomalies with opposite sign around equatorial Africa. This pair of coupled patterns for the first mode implies that when the monsoon rainfall from tropical Africa to India becomes more intense (i.e. the OLR anomaly is negative), the upper troposphere becomes warmer than normal over the areas from northern Africa to western Asia and along southern subtropics covering southern Africa.

- The temperature variation in the middle and upper troposphere over the Eurasian continent (especially western Eurasia) during the summer monsoon season is shown to be the result of the Asian-African monsoon rainfall anomaly. The atmospheric circulation anomaly induced by enhanced tropical heating with the intensified monsoon rainfall facilitates the warming over western Eurasia through the large-scale subsidence and warm thermal advection resulting from the response of stationary Rossby waves to the near-equatorial thermal forcing.

This work was originally motivated to find the impact of year-to-year variations of the TT related to Eurasian land surface temperature on the variability of the Asian summer monsoon. However, what became evident is the robust effect of the varying monsoonal rainfall upon the variability of TT on a planetary scale. The upper TT in the subtropics is highly correlated with the varying monsoonal rainfall through dynamical responses of the atmosphere to the released heat of condensation associated with the rainfall. Previous investigations (e.g. Li and Yanai 1996; Kawamura 1998) showed that there is a close relationship between the TT and the Asian monsoon. However, the present study indicates that the summer TT over Eurasia is to a great extent a response to the rainfall anomaly related to the Asian-African monsoon. The influence of the monsoon rainfall on TT over western Eurasia is confirmed to be a manifestation of the mechanism of the desert dynamics proposed by Rodwell and Hoskins (1996) in the temperature field on an interannual time-scale.

Although we detect some precursory springtime temperature signals in upper TT over Eurasia, especially near India, there is a suggestion that the variation in the upper TT is independent from that of the land surface temperature. Based on our correlation analysis related to SST and the results from previous modelling studies (Shen *et al.* 1998; Lau and Nath 2000), we speculate that the MAM temperature anomaly in the upper troposphere, which can be used as a precursor signal of an anomalous monsoon, may actually result from the SST in the equatorial Pacific and simultaneous tropical rainfall anomalies. The springtime TT anomaly, once established, will promote the anomaly of the following summer monsoon. This speculation needs to be validated in the future with more detailed analyses and related numerical experiments. At this stage, however, we should not entirely exclude the role of the land surface processes in

modulating the monsoon variability. The impact of land surface conditions such as soil moisture and snow cover may have subtle effects upon the timing of monsoon onset. Revealing such effects will be a goal of the authors' future work.

ACKNOWLEDGEMENTS

The authors are grateful to two anonymous reviewers for their valuable comments and suggestions for improving this paper. They acknowledge the NCEP, the Indian Institute of Tropical Meteorology and the Climatic Research Unit, University of East Anglia for providing the datasets used in the present study, and the beneficial discussions with A. Arakawa, J.-L. Li, and J.-Y. Yu. They also thank Wen-wen Tung for her help in many aspects of this work. This work was supported by the NOAA Office of Global Programs under Grant NA96GP0331.

REFERENCES

- Bretherton, C. S., Smith, C. and Wallace, J. M. 1992 An intercomparison of methods for finding coupled patterns in climate data. *J. Climate*, **5**, 541–560
- Broccoli, A. J. and Manabe, S. 1992 The effects of orography on middle latitude northern hemisphere dry climates. *J. Climate*, **5**, 1181–1201
- Charney, J. G. 1975 Dynamics of deserts and drought in the Sahel. *Q. J. R. Meteorol. Soc.*, **101**, 193–202
- Fennessy, M. J. and Shukla, J. 1999 Impact of initial soil wetness on seasonal atmospheric prediction. *J. Climate*, **12**, 3167–3180
- Flohn, H. 1957 Large-scale aspects of the 'summer monsoon' in south and east Asia. *J. Meteorol. Soc. Jpn.*, (75th Ann. Vol.), 180–186
- Fu, C. and Fletcher, J. O. 1985 The relationship between Tibet tropical ocean thermal contrast and interannual variability of Indian monsoon rainfall. *J. Clim. Appl. Meteorol.*, **24**, 841–847
- Gill, A. E. 1980 Some simple solutions for heat-induced tropical circulation. *Q. J. R. Meteorol. Soc.*, **106**, 447–462
- He, H., McGinnis, J. W., Song, Z. and Yanai, M. 1987 Onset of the Asian summer monsoon in 1979 and the effect of the Tibetan Plateau. *Mon. Weather Rev.*, **115**, 1966–1995
- Jones, P. D. 1994 Hemispheric surface air temperature variations: A reanalysis and an update to 1993. *J. Climate*, **7**, 1794–1802
- Kalnay, E., Kanamitsu, M., Kistler, R., Collins, W., Deaven, D., Gandin, L., Iredell, M., Saha, S., White, G., Woollen, J., Zhu, Y., Chelliah, M., Ebisuzaki, W., Higgins, W., Janowiak, J., Mo, K. C., Ropelewski, C., Wang, J., Leetmaa, A., Reynolds, R., Jenne, R. and Joseph, D. 1996 The NCEP/NCAR 40-year reanalysis project. *Bull. Am. Meteorol. Soc.*, **77**, 437–471
- Kawamura, R. 1998 A possible mechanism of the Asian summer monsoon–ENSO coupling. *J. Meteorol. Soc. Jpn.*, **76**, 1009–1027
- Krishnan, R. and Mujumdar, M. 1999 Remotely and regionally forced pre-monsoon signals over northern India and neighbourhood. *Q. J. R. Meteorol. Soc.*, **125**, 55–78
- Lau, K. M. and Bua, W. 1998 Mechanisms of monsoon Southern Oscillation coupling: Insights from GCM experiments. *Clim. Dyn.*, **14**, 759–779
- Lau, N.-C. and Nath, M. J. 2000 Impact of ENSO on the variability of the Asian–Australian monsoons as simulated in GCM experiments. *J. Climate*, **13**, 4287–4309
- Li, C. and Yanai, M. 1996 The onset and interannual variability of the Asian summer monsoon in relation to land–sea thermal contrast. *J. Climate*, **9**, 358–375
- Matsuno, T. 1966 Quasi-geostrophic motions in the equatorial areas. *J. Meteorol. Soc. Jpn.*, **44**, 25–43

- Meehl, G. A. 1994 Coupled land-ocean-atmosphere processes and south Asian monsoon variability. *Science*, **266**, 263-267
- 1997 The south Asian monsoon and the tropospheric biennial oscillation. *J. Climate*, **10**, 1921-1943
- Mooley, D. A., Parthasarathy, B., Sontakke, N. A. and Munot, A. A. 1981 Annual rain-water over India, its variability and impact on the economy. *J. Climatol.*, **1**, 167-186
- Ogasawara, N., Kitoh, A., Yasunari, T. and Noda, A. 1999 Tropospheric biennial oscillation of the ENSO-monsoon system in the MRI coupled GCM. *J. Meteorol. Soc. Jpn.*, **77**, 1247-1270
- Ose, T. 1996 The comparison of the simulated response to the regional snow mass anomalies over Tibet, eastern Europe, and Siberia. *J. Meteorol. Soc. Japan*, **74**, 845-866
- Parthasarathy, B., Sontakke, N. A., Munot, A. A. and Kothawale, D. R. 1987 Droughts/floods in the summer monsoon rainfall season over different meteorological subdivisions of India for the period 1871-1984. *J. Climatol.*, **7**, 57-70
- Rodwell, M. and Hoskins, B. 1996 Monsoons and the dynamics of deserts. *Q. J. R. Meteorol. Soc.*, **122**, 1385-1404
- Sankar-Rao, M., Lau, K. M. and Yang, S. 1996 On the relationship between Eurasian snow cover and the Asian summer monsoon. *Int. J. Climatol.*, **16**, 605-616
- Shen, X., Kimoto, M. and Sumi, A. 1998 Role of land surface processes associated with interannual variability of broad-scale Asian summer monsoons as simulated by the CCSR/NIES AGCM. *J. Meteorol. Soc. Jpn.*, **76**, 217-236
- Singh, G. P. and Chattopadhyay, J. 1998 Relationship of tropospheric temperature anomaly with Indian southwest monsoon rainfall. *Int. J. Climatol.*, **18**, 759-763
- Ueda, H. and Yasunari, T. 1998 Role of warming over the Tibetan Plateau in early onset of the summer monsoon over the bay of Bengal and the south China sea. *J. Meteorol. Soc. Jpn.*, **76**, 1-12
- Vernekar, A. D., Zhou, J. and Shukla, J. 1995 The effect of Eurasian snow cover on the Indian monsoon. *J. Climate*, **8**, 248-266
- Wallace, J. M., Smith, C. and Bretherton, C. S. 1992 Singular value decomposition of wintertime sea surface temperature and 500-mb height anomalies. *J. Climate*, **5**, 561-576
- Watanabe, M. and Nitta, T. 1998 Relative impacts of snow and sea surface temperature anomalies on an extreme phase in the winter atmospheric circulation. *J. Climate*, **11**, 2837-2857
- Webster, P. J. 1972 Response of the tropical atmosphere to local steady forcing. *Mon. Weather Rev.*, **100**, 518-541
- Webster, P. J., Magana, V. O., Palmer, T. N., Shukla, J., Tomas, R. A., Yanai, M. and Yasunari, T. 1998 Monsoons: Processes, predictability, and the prospects for prediction. *J. Geophys. Res.*, **103**, 14451-14510
- Webster, P. J. and Yang, S. 1992 Monsoon and ENSO—selectively interactive systems. *Q. J. R. Meteorol. Soc.*, **118**, 877-926
- Xie, P. P. and Arkin, P. A. 1997 Global precipitation: A 17-year monthly analysis based on gauge observations, satellite estimates, and numerical model outputs. *Bull. Am. Meteorol. Soc.*, **78**, 2539-2558
- Yanai, M., Li, C. and Song, Z. 1992 Seasonal heating of the Tibetan Plateau and its effects on the evolution of the Asian summer monsoon. *J. Meteorol. Soc. Jpn.*, **70**, 319-351
- Yang, S. and Lau, K. M. 1998 Influences of sea surface temperature and ground wetness on Asian summer monsoons. *J. Climate*, **11**, 3230-3246
- Yasunari, T. and Seki, Y. 1992 Role of the Asian monsoon on the interannual variability of the global climate system. *J. Meteorol. Soc. Jpn.*, **70**, 177-189
- Yeh, T.-C., Luo, S.-W. and Chu, P.-C. 1957 The wind structure and heat balance in the lower troposphere over Tibetan Plateau and its surroundings. *Acta Meteorol. Sinica*, **28**, 108-121 (in Chinese)
- Zwiers, F. W. 1993 Simulation of the Asian summer monsoon with the CCC GCM-1. *J. Climate*, **6**, 470-486